An optical study of silicate glass containing Cr^{3+} and Cr^{6+} ions

1996 J. Phys.: Condens. Matter 8 9059

(http://iopscience.iop.org/0953-8984/8/46/011)

J. Phys.: Condens. Matter **8** (1996) 9059–9069. Printed in the UK

An optical study of silicate glass containing Cr^{3+} and Cr^{6+} ions

M Casalboni†, V Ciafardone†, G Giuli‡, B Izzi†, E Paris‡ and P Prosposito§

† Dipartimento di Matematica e Fisica, e Istituto Nazionale di Fisica della Materia, Università di Camerino, Via Madonna delle Carceri, 62032 Camerino (MC), Italy

‡ Dipartimento di Scienze della Terra, e Istituto Nazionale di Fisica della Materia, Università di Camerino, Via Gentile III da Varano, 62032 Camerino (MC), Italy

§ Dipartimento di Fisica, e Istituto Nazionale di Fisica della Materia, Università di Roma Tor Vergata, Via della Ricerca Scientifica, 1, 00133 Roma, Italy

Received 15 April 1996, in final form 25 July 1996

Abstract. The optical properties of chromium-doped sodium silicate glass synthesized under oxidizing conditions have been investigated. The method of preparation provides a large concentration of Cr^{6+} ions, but absorption and emission spectra showed that a small amount of Cr^{3+} (and Cr^{5+}) ions are always present. The Dq-, B- and C-parameters of the crystal-field theory for the Cr^{3+} ion were obtained, confirming the glassy nature of the sample. Cr^{3+} luminescence was observed in the near-infrared region, even at room temperature, confirming the low value of the crystal-field Dq. Moreover, the high ultraviolet transparency of this matrix allows observation of a well resolved absorption spectrum of the Cr^{6+} ion.

1. Introduction

In the last three decades a great effort has been devoted to the study of glasses containing transition metal and rare-earth element impurities [1–3]. One of the most investigated impurity ions is Cr^{3+}, and the large number of review articles and papers testifies to the high level of interest in this field [4–6], even in connection with the development of lasers. Currently, the basic features of Cr^{3+} in a large number of crystalline matrices are so well established that this ion is extensively used as a *probe* for studying the structure and the local symmetry of new and exotic materials.

Moreover, in applications ranging from new optical material research to optoelectronic and integrated optical devices, there is an increasing interest in glasses, due to their lower production costs with respect to single crystals.

In this regard an interesting point is whether the host matrix is fully glassy or some crystallites are present. In this regard also, the study of the optical properties of the Cr^{3+} ions can help to solve the problem. In fact, the optical properties of ion impurities in glasses show differences with respect to the corresponding crystalline matrices. In particular, the emission properties in the glass are characterized by broader emission spectra, a radiation lifetime with a non-exponential decay law and a peculiar temperature dependence of the quantum efficiency [7].

In nature chromium is known to occur both as Cr^{6+} and Cr^{3+}. In minerals, the first is found to be tetrahedrally coordinated by oxygen as $[CrO_4]^{2-}$ or $[Cr_2O_7]^{2-}$ with Cr–O mean distances ranging from 1.60 to 1.67 Å. Cr^{3+} favours instead distorted octahedrally

0953-8984/96/469059+11$19.50

coordinated environments (as in Cr_2O_3), with Cr–O mean distances from 1.97 to 2.00 Å. In melts, physical properties such as density and viscosity are affected by the degree of polymerization and therefore it is important to investigate the structural role of all of the components, especially of the transition elements which may occur in these systems with different valence and local geometry. Silicate melts can be synthesized, quenched to glass and studied by a variety of spectroscopic methods in order to better understand the melt structure and coordination environments of different melt components. The information gained on Cr will relate to both the oxidation state and the local geometry.

In fact it is of interest to evaluate whether Cr occurs in polyhedra tetrahedrally or octahedrally coordinated with oxygen; in the first case it may act as a network-forming species and increases the polymerization degree of the melt, whereas in the second case it may behave as a network modifier, interrupting the chains of SiO_4 tetrahedral units. From the point of view of the earth sciences, this information can give a better knowledge of the physics and chemistry of magmas.

In this paper we point out the possibility of hosting easily impurity ions with different valence in a glassy matrix. We investigate here a Cr-doped sodium silicate glass that shows an excellent ultraviolet transmission, having an intrinsic absorption edge in the region of 5 eV. This allows us to extend the analysis up to 4.5 eV, well above the region where the absorption attributed to the charge-transfer transitions of Cr^{6+} occurs. Moreover, silicate glasses show higher emission quantum efficiency with respect to fluoride glasses [6], opening up new possibilities in the exploitation of these materials as active elements in laser and in optoelectronic devices.

2. Experimental results

The samples were synthesized using the following procedure: a mixture of oxides and carbonates in suitable amounts (3 mol of SiO_2 and 1 mol of Na_2CO_3) was finely ground together with 3% (molar) of Cr_2O_3 and held at 120 °C for 24 hours to dehydrate. The dried mixture was then put in a platinum crucible held at 900 °C for several hours in order to de-carbonate, and then melted at 1675 °C in air. This process produces a consistent amount of Cr^{6+}. The rapid quench to room temperature was the last step for producing the glass. The amorphicity and homogeneity of the samples has been checked under the optical microscope using a suitable immersion oil.

Samples with lower Cr concentration were produced by means of dilution of the original glass. The sample containing 3% of Cr_2O_3 was remelted with a suitable amount of undoped material. In this way we obtained two other samples with nominal 1% and 0.1% Cr_2O_3 content. An undoped glass sample was also synthesized to be used for comparison as a blank reference.

The absorption spectra were recorded by means of a commercial spectrophotometer fitted with a closed-cycle cryostat in order to hold the sample temperature at fixed values between 20 and 300 K. The spectral range investigated was 190–3000 nm.

The absorption spectra of the 1% Cr_2O_3-doped sample taken at 20 and 300 K, as well as that of the undoped sample show a transmission range larger than that of other glasses and crystals [1] (figure 1). The doped samples were cut from larger ingots, ground down to 0.5 mm in thickness and the surfaces were polished in order to decrease the influence of the light scattering. The dominant feature in the spectra of the Cr-doped sample is a large band at around 3.4 eV, a smaller one below 2 eV and some features between 2.5 and 3.0 eV. The absorption bands do not change as the temperature increases up to room temperature (RT). A slight difference on the high-energy side between doped and undoped materials

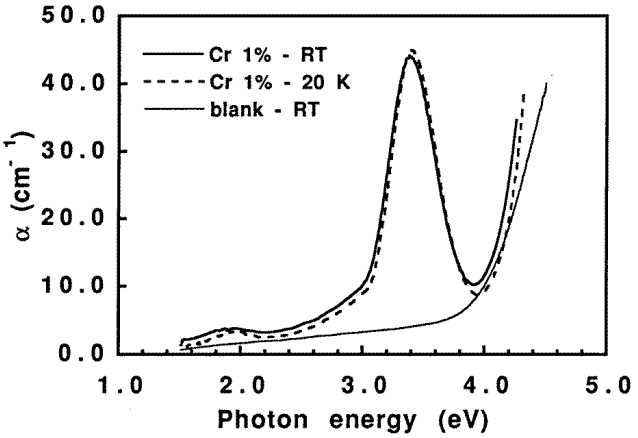

Figure 1. Absorption spectra of the sodium silicate glass containing 1% Cr_2O_3 taken at 300 and 10 K. The thin line shows the absorption spectra of the blank sample.

could depend on the unequal polishing of the sample surfaces producing different amounts of scattering.

More detailed measurements were performed on samples with different Cr contents in order to assign the absorption bands (see below).

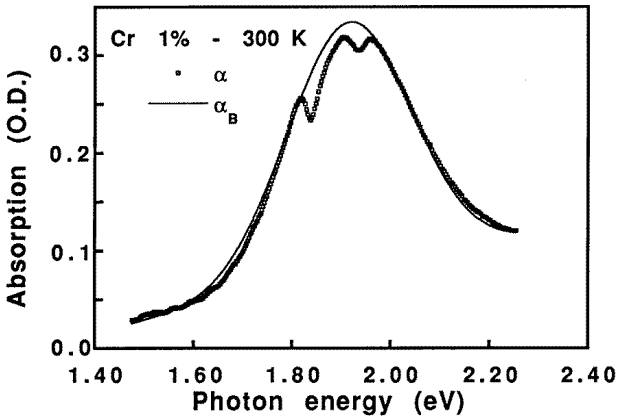

Figure 2. The absorption spectrum of the sodium silicate glass containing 1% Cr_2O_3 taken at 300 K. The continuous line represents the fit of the absorption wings for extracting the background gaussian-shaped band (see the text for details).

In figure 2 we show the absorption spectrum, taken at 300 K, of the lowermost energy band of the 1% Cr_2O_3 sample. It shows the characteristic shape of the Cr^{3+} ($^4A_2 \rightarrow {}^4T_2$) absorption. The structures that modify the gaussian line shape are due to Fano antiresonances that appear when a large band and narrow lines are superimposed in the same energy region. In the present case the large absorption band is due to the $^4A_2 \rightarrow {}^4T_2$ transition while the narrower $^4A_2 \rightarrow {}^2E$ and $^4A_2 \rightarrow {}^2T_1$ transitions produce the modulation of the shape. In figure 2 we also report (continuous line) the gaussian best fit obtained using the experimental

data. In order to minimize the effect of the Fano notches on the determination of the $^4A_2 \rightarrow {}^4T_2$ band parameters, we masked the Fano-related experimental points during the least-squares fitting procedure.

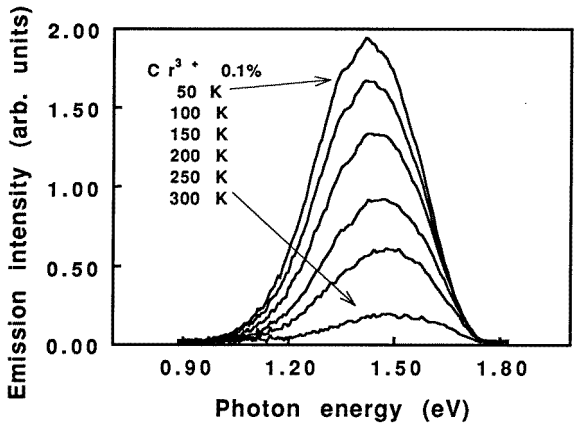

Figure 3. Emission spectra of the sodium silicate glass containing 0.1% Cr_2O_3 excited by a He–Ne laser (λ = 632.8 nm), taken at different temperatures.

In figure 3 we show the emission spectra, taken at different temperatures, of the 0.1% Cr_2O_3-doped sample excited with an 5 mW He–Ne laser ($\lambda = 632.8$ nm). The spectra were corrected for the spectral dependence of the apparatus by means of a calibration procedure based on a known source (black body). The emission intensity is strongly temperature dependent, as in most transition-metal-ion impurities, and it shows a remarkable blue-shift as the temperature rises.

3. Discussion

The experimental data cannot be interpreted in terms of Cr^{3+} alone, but have to be analysed in view of the coexistence of Cr ions of different valences. However, as witnessed by the shape and energy position of the lowermost absorption band, Cr^{3+} is present in all samples produced. We now begin to discuss this point.

The Cr^{3+} free ion has an external configuration with three equivalent d electrons giving ^4F, ^4P and ^2G spectral terms. When the ion is incorporated into a solid matrix (crystal or glass) the states are modified, due mainly to interaction with six nearest-neighbour atoms (ligand atoms). It is be noted that the symmetry of the CrO_6 complex remains octahedral or slightly distorted octahedral, independently of the crystallinity of the matrix. The metal–ligand interaction can be theoretically described by means of a molecular orbital picture applied to the CrO_6 complexes or of cluster model [8, 9]. However, the energy values of the Cr^{3+} multiplet observed experimentally can be fitted using suitable parameters into the crystal-field scheme [4, 5, 8].

3.1. Absorption spectra

Significant parameters of this theory include the crystal-field Dq-parameters and the Racah parameters B and C, which can be evaluated from optical absorption transitions. In

particular, the value of the crystal-field Dq is given by the energy difference between the ground and first excited state of the Cr^{3+}, $^4A_2$ and $^4T_2$ respectively, and the result, for our samples, is

$$Dq = \frac{E(^4T_2) - E(^4A_2)}{10} = 194 \pm 1 \text{ meV}. \tag{1}$$

In order to evaluate the relevant B-parameter we have to disentangle the higher-energy side of the absorption spectrum. The value of the Racah B-parameter can be estimated from the position of the two lowest-lying absorption bands:

$$\frac{Dq}{B} = \frac{15(x-8)}{x^2 - 10x} \tag{2}$$

with

$$x = \frac{E(^4A_2 \rightarrow {}^4T_1) - E(^4A_2 \rightarrow {}^4T_2)}{Dq}. \tag{3}$$

In order to solve this equation we need the energy position of the $^4A_2 \rightarrow {}^4T_1$ transition. This transition is expected to be in the 2.4 to 3.0 eV range in order to have a B-value compatible with literature data for crystals and glasses. Unfortunately the related absorption band is hidden by the low-energy wing of the 3.4 eV band, so we can obtain information only by means of a fitting procedure.

First of all we try to fit the experimental absorption data by means of a unique gaussian band in the 2.5–3.2 eV region. The energy position of the $^4A_2 \rightarrow {}^4T_1$ transition so estimated led to the value $Dq/B \sim 2.8$, completely inconsistent with the emission findings (see below). Moreover, in samples with different Cr contents, the relative height of the band so obtained with respect to the well resolved $^4A_2 \rightarrow {}^4T_2$ band was not constant.

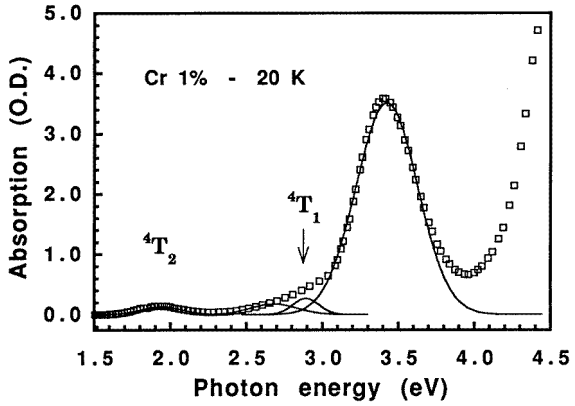

Figure 4. The absorption spectrum of the sodium silicate glass containing 1% Cr_2O_3 at 20 K. Continuous lines show the gaussian components of the spectrum obtained as a result of the fitting procedure.

For these reasons, we tried to fit the data with two gaussian curves in the intermediate-energy region. Figure 4 shows the best fit of the Cr 1% sample absorption spectrum recorded at 20 K. The fitting parameters (reported in table 1) yield a constant height ratio between the 1.94 and 2.90 eV bands for all the samples on which measurements were made. Substituting the best-fit peak energies into equations (2) and (3) yields $x = 5.0 \pm 0.1$ and a B-value of 106 ± 5 meV.

Table 1. Fitting parameters of the absorption spectra with gaussian bands. The intensities are related to the spectra of figure 4. The peak energy and half-width values are obtained as averages of low-temperature spectra of different samples.

Band	Intensity (arbitrary units)	Peak energy (eV)	Half-width (eV)	Transition
I	0.13	1.94 ± 0.01	0.33 ± 0.03	Cr^{3+} ($^4A_2 \rightarrow {}^4T_2$)
II	0.18	2.68 ± 0.01	0.42 ± 0.04	Cr^{5+}
III	0.27	2.90 ± 0.01	0.25 ± 0.03	Cr^{3+} ($^4A_2 \rightarrow {}^4T_1$)
IV	3.51	3.44 ± 0.01	0.50 ± 0.03	Cr^{6+}

The Racah C-parameter can be evaluated if we exploit the Fano structures (figure 2), which are related to the $^4A_2 \rightarrow {}^2E$ and $^4A_2 \rightarrow {}^2T_2$ transitions. On the basis of investigations by Sturge *et al* [10], Lempicki *et al* [3] and Voda *et al* [11], we fit the ratio between the experimental data and the so-called *background* α_B of figure 2, i.e. the undistorted gaussian shape obtained by a best fit of both wings of the structure, in order to exclude the effect of the Fano notches. Various trials with different values of α_B were made. However, the relevant parameter obtained did not depend significantly on the choice of the background shape.

Table 2. Parameters of the fitting of the Fano structures. Details are given in the text.

Transition	ρ^2	q (eV)	ω_{ir} (eV)	γ
$^4A_2 \rightarrow {}^2E$	0.088	−0.372	1.84	0.0145
$^4A_2 \rightarrow {}^2T_1$	0.037	0.190	1.94	0.015

Figure 5 shows the experimental data and their fit to the expression

$$R(\omega) = 1 + \rho_1^2 \frac{q_1^2 + 2q_1\epsilon_1 + 1}{1 + \epsilon_1^2} + \rho_2^2 \frac{q_2^2 + 2q_2\epsilon_2 + 1}{1 + \epsilon_2^2} \tag{4}$$

where

$$\epsilon_i = \frac{\omega - \omega_{ri}}{\gamma_i}. \tag{5}$$

$\hbar\omega_{ri}$ is the energy of the discrete level perturbed by the interaction with the pseudo-continuum and γ_i^{-1} is related to the lifetime of the same level. The ρ^2-parameter (p in the notation of [10] and [11]) gives the fraction of continuum states $^4T_2$ interacting with sharp levels via spin–orbit coupling, and the q-parameter, ranging from $-\infty$ to $+\infty$, characterizes the line shape: the closer to zero the value of $|q|$, the more similar to an antiresonance (notch) is the line profile. The resulting parameters are reported in table 2.

From the energy position of the ^2E level we can evaluate the C-parameter, following Rasheed *et al* [4]:

$$\frac{C}{B} = \frac{1}{3.05}\left[\frac{E(^2E)}{B} - 7.9 + 1.8\left(\frac{B}{Dq}\right)\right] = 3.4. \tag{6}$$

Table 3 summarizes the parameter values. Using them we draw the Tanabe–Sugano diagram for Cr^{3+} in this glass, shown in figure 6. It indicates the general behaviour of the Cr^{3+}-ion energy levels as a function of the local field strength measured in terms of Dq/B.

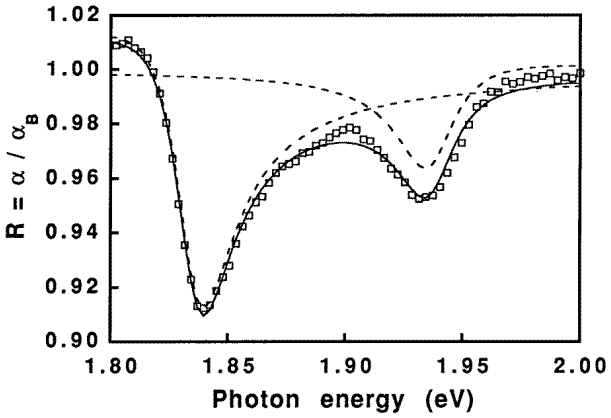

Figure 5. Fano structures obtained from the ratio between the experimental data of the absorption spectrum and the background gaussian shape. The broken line gives the best fit according to equation (4).

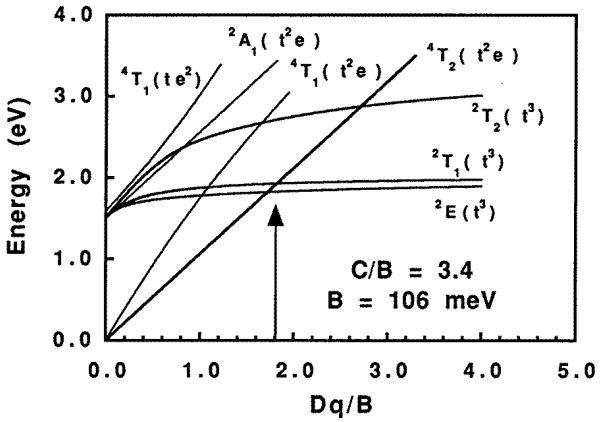

Figure 6. The Tanabe–Sugano diagram of Cr^{3+} in sodium silicate glass obtained with the fitted parameter $C/B = 3.4$. The arrow shows the field obtained.

Table 3. Crystal-field parameters of the Cr^{3+} ion in sodium silicate glass.

Dq (eV)	0.194 ± 0.001
Dq/B	1.8 ± 0.1
B (eV)	0.106 ± 5
C (eV)	0.360 ± 20
C/B	3.4

The arrow shows the value of the local field obtained by means of the above analysis for this material. The value turns out to be rather low in comparison with that obtained for crystals and other glasses. This value suggests a high value of the ligand–Cr distance R as given by the relation $Dq \propto R^{-n}$ with n near 5 as obtained theoretically [12, 13] and experimentally by means of optical measurements at variable pressure [14]. Moreover the

value of Dq/B is found to be in an intermediate region, close to the crossing point between $^4T_2$ and the field-independent ^2E and $^2T_1$ energy curves. This implies broad-band emission and possible tiny narrow emission lines, but despite our careful measurements no narrow emission lines were observed.

We have to attribute the origin of the other band resulting from the fitting procedure, whose peak is at around 2.7 eV.

An attribution of the band located at about 2.7 eV to the $^4A_2 \rightarrow {}^2T_2$ (t^3) transition of the Cr^{3+} ion is to be ruled out due to its large bandwidth in contrast with the low dependence of the energy position of this transition upon the crystal field. Moreover the relative height of this band with respect to the other Cr^{3+}-related absorption bands is not constant for different samples.

The band at 2.7 eV could be due to chromium in different valence states. However, Cr^{4+} seems to be ruled out because this ion shows in forsterite (Mg_2SiO_4) [15–17], absorption bands at 1.2 and 2.0 eV. On the other hand Cr^{5+} has an absorption band at around 2.8 eV in SiO_2 glass [18].

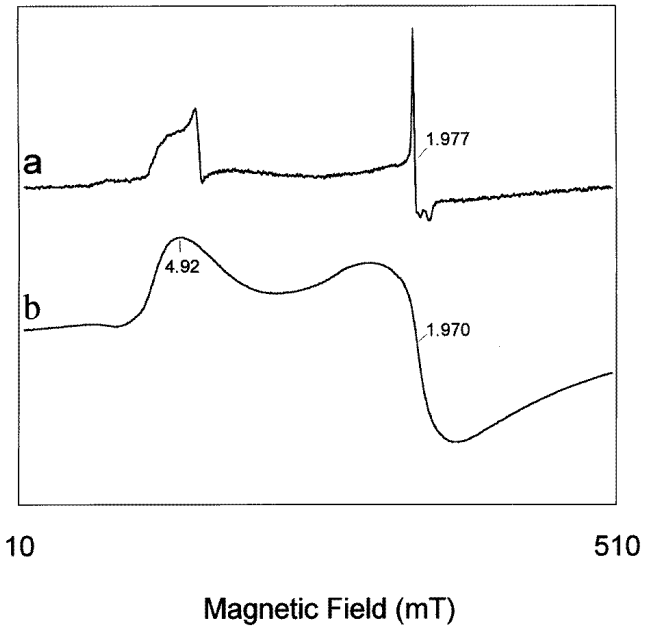

Figure 7. EPR spectra at 77 K for glass containing 1% (top) and 3% (bottom) Cr_2O_3.

In order to definitively attribute this band, and to obtain information about the strong absorption at 3.4 eV, we performed EPR studies at 77 K for all of the samples. In figure 7 we report the EPR spectra of the samples with nominal 1% (top) and 3% (bottom) Cr_2O_3 contents. In the first spectrum one observes, in the low-field region, the signal of Cr^{5+} with $g = 1.977$ and a linewidth of 25 G superimposed with the Cr^{3+} signal ($g = 1.970$ and a linewidth of about 700 G) [19]. In the high-field region one can observe a $g = 4.92$ signal due to Cr^{3+} and a $g = 4.3$ signal due to iron (an unwanted impurity present also in the Cr-undoped glass). The spectrum is similar to that recently reported [20, 21] for a biological system in which Cr^{3+} and Cr^{5+} are simultaneously present. On increasing the Cr concentration (bottom of figure 7) the signal originating from Cr^{3+} dominates and hides

all the other signals [19].

The 3.4 eV band, that is always present in the optical spectra as the most prominent feature, and that turns out to be not correlated to any of the EPR structures, can be attributed to the EPR-invisible Cr^{6+} ion and in particular to a Cr^{6+} charge-transfer transition. Few data have been reported on this band in glasses. Smith and Cohen [1] observed absorption bands at 3.37 and 4.68 eV in $(Na_2O)_{0.3}(SiO_2)_{0.7}$ glass containing 0.37% Cr when prepared in oxidizing conditions and they attribute the bands to Cr^{6+}. More recently, Rasheed *et al* [4] reported a strong charge-transfer band at about 3.44 eV due to Cr^{6+} ions in commercial ED-2 glass containing Cr_2O_3.

An absorption band in the high-energy region was also observed in heavily doped silica coatings fabricated via the sol–gel method $[(Cr_2O_3)_{0.2}(SiO_2)_{0.8}]$ [22]. The authors attribute the 3.35 eV absorption band to Cr^{6+} in tetrahedral sites. Similar data were presented by Duran *et al* [23] and Ohta and Kurokawa [24]. The latter reference reports the presence of the high-energy absorption bands in samples annealed at high temperature in air.

Charge-transfer spectra can arise from transitions involving the excitation of an electron from an electronic state of the host crystal to a final state of the substitutional metal ion. These transitions are generally fully allowed and the related absorption spectra consist of intense bands at high energy [26, 28].

An estimation of their energy positions can be given following the phenomenological theory by Jørgensen [25] making use of the relation

$$E_{CT}\ (\mathrm{eV}) = 3.72[x_{opt}(\mathrm{X}) - x_{opt}(\mathrm{M})] \tag{7}$$

where E_{CT} is the energy position of the absorption peak of the charge-transfer transition, and $x_{opt}(\mathrm{X})$ and $x_{opt}(\mathrm{M})$ are the optical electronegativities of the ligand and the metal ion respectively. Taking into account the estimated value for the optical electronegativity for the oxides ($x_{opt} \sim 3.1$) and its linear dependence upon the number of electrons for the metal ion [25], we obtain for E_{CT} a value of about 3.8 eV that agrees fairly well with the experimental value of 3.4 eV.

The absorption band is very insensitive to changes of temperature: only a small red-shift of the peak energy ($\Delta E \sim 20$ meV) was observed from 10 K to RT, while the half-width and the height of the band remain unchanged, at least within the limits of the experimental error.

This behaviour is in contrast with that observed for other charge-transfer transitions in fluoride crystals [27], showing an energy difference of 200 meV from RT to 10 K. However, Tippins [28] did not observe any difference in energy position and width of the bands in Al_2O_3 between the RT and LNT spectra. Moreover our bandwidth result is 0.50 ± 0.01 eV, similar to the value of 0.7 eV reported in [28].

The comparison among samples with different Cr contents shows that the relative concentration of Cr^{3+} and Cr^{6+} varies, the former being preferred in more diluted samples.

3.2. Emission spectra

The emission spectra shown in figure 3 are characterized by a broad band, whose intensity decreases on increasing the temperature due to a non-radiative transition toward the ground state. An Arrhenius plot for this process yields an activation energy of 11 meV. We point out that higher quantum efficiency was obtained for lower Cr concentration. This concentration quenching of the luminescence was recently reported [29] together the well known multiexponential decay time always observed for disordered [30] and glassy [31–33] systems.

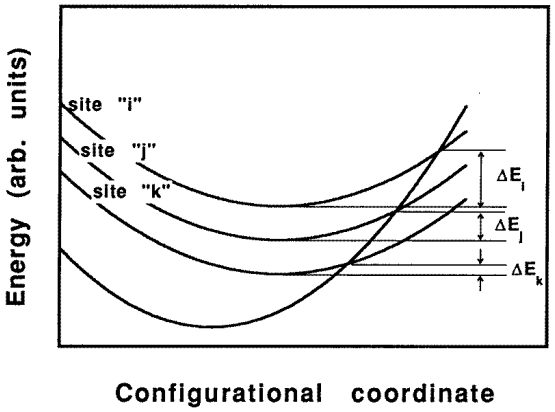

Figure 8. A schematic representation of the mechanism of the blue-shift of the emission band. As the temperature rises the non-radiative transitions from the lower parabolae towards the ground state became more and more probable.

Our observation of the evident blue-shift of the emission spectrum as the temperature rises is similar to the behaviour observed by Yamaga *et al* [7] for silicate glasses containing Cr^{3+}, which was related to site distribution of the excited-state energy. As the temperature increases the excited states with lower energy (responsible for the lower-energy side of the emission band) can perform a non-radiative transition toward to the ground state leading to a change of the shape of the emission band. Figure 8 shows a configurational coordinate scheme with different excited-state parabolae, indicated by the letters i, j, k, ..., related to different environmental sites for the Cr^{3+} ion. It shows that all of the parabolae are populated at the same time and thermal population does not play any role in producing jumps among them. Each relaxed excited state (RES) can be coupled to the ground state via a non-radiative transition with probability k_i, k_j, k_k, ..., with $k_i < k_j < k_k$ due to the different values of the barrier height ΔE. As the temperature rises the more probable non-radiative de-excitation involves the lower-lying parabolae. The consequence of this process is an apparent blue-shift resulting in the displacement of the *centre of gravity* of the convolution of different component emissions.

Attempts were made to reveal luminescence excited in the 3.4 eV absorption band, but no emission was observed.

4. Conclusions

Absorption and emission measurements of silicate glass containing mixed-valence chromium allow a quantitative analysis for the octahedrally coordinated Cr^{3+} and this reveals a low value of the local field ($Dq/B \sim 1.80$), as confirmed by broad-band emission.

The emission behaviour as a function of temperature and its blue-shift are typical of disordered systems. Moreover the presence of a broad emission band in the near-infrared region, observable even at room temperature, could be of interest, due to the easy synthesis of this material.

Due to the high UV transparency of the matrix it was possible to observe an absorption band attributed to Cr^{6+}. No emission was observed on excitation of this band.

Acknowledgments

The authors thank the Bayerisches Geoinstitut under the EC Human Capital and Mobility–Access to Large Scale Facilities for glass syntheses. They also thank Michael R Carrol, Roberto Francini and Umberto M Grassano for helpful discussions and Francesca Polizio for the EPR measurements. They thank Roberto Bernardini for technical assistance during the emission measurements.

References

[1] Smith H L and Cohen A J1963 *Phys. Chem. Glasses* **4** 173
[2] Schultz P C 1974 *J. Am. Ceram. Soc.* **57** 307
[3] Lempicki A, Andrews L, Nettel S J, McCollum B C and Solomon E I 1980 *Phys. Rev. Lett.* **44** 1234
[4] Rasheed F, O'Donnell K P, Henderson B and Hollis D B 1991 *J. Phys.: Condens. Matter* **3** 1915
[5] Rasheed F, O'Donnell K P, Henderson B and Hollis D B 1991 *J. Phys.: Condens. Matter* **3** 3825
[6] Balda R, Fernández J, Elejalde M J, Illarramendi M A and Jacoboni C 1991 *J. Phys.: Condens. Matter* **3** 7695
[7] Yamaga M, Henderson B, O'Donnell K P and Gao Y 1991 *Phys. Rev.* B **44** 4853
[8] Luaña V, Bermejo M, Flòrez M, Recio J M and Pueyo 1989 *J. Chem. Phys.* **90** 6409
[9] Groh D J, Pandey R and Recio J M 1994 *Phys. Rev.* B **50** 14 860
[10] Sturge M D, Guggenheim H J and Pryce M H L 1970 *Phys. Rev.* B **2** 2459
[11] Voda M, García Solé J, Jaque F, Vergara I, Kaminskii A, Mill B and Butashin A 1994 *Phys. Rev.* B **49** 3755
[12] Moreno M, Barriuso M T and Aramburu J A 1992 *J. Phys. C: Solid State Phys.* **4** 9481
[13] Marco de Lucas M C, Rodríguez F and Moreno M 1994 *Phys. Rev.* B **50** 2760
[14] Duclos S J, Vohra Y K and Ruoff A L 1990 *Phys. Rev.* **41** 5372
[15] Moncorgé R, Cormier G, Simkin D J and Capobianco J A 1991 *IEEE J. Quantum Electron.* **27** 114
[16] Jia Weiyi, Liu Huimin, Jaffe S, Yen W M and Denker B 1991 *Phys. Rev.* B **43** 5234
[17] Moncorgé R, Manaa H and Boulon G 1994 *Opt. Mater.* **4** 139
[18] Herren M, Nishiuchi H and Morita M 1994 *J. Chem. Phys.* **101** 4461
[19] Landry R J, Fournier J T and Young C G 1967 *J. Chem. Phys.* **46** 1285
[20] Sugiyama M and Tsuzuki K 1994 *FEBS Lett.* **341** 273
[21] Sugiyama M 1994 *Environmental Health Perspect.* **102** 31
[22] Orgaz F and Rawson H 1986 *J. Non-Cryst. Solids* **82** 378
[23] Duran A, Fernandez Navarro J M, Mazon P and Joglar A 1988 *J. Non-Cryst. Solids* **100** 494
[24] Ohta H and Kurokawa Y 1992 *J. Mater. Sci. Lett.* **11** 868
[25] Jørgensen C K 1971 *Modern Aspects of Ligand Field Theory* (Amsterdam: North-Holland)
[26] Di Bartolo B 1968 *Optical Transitions of Ions in Solids* (New York: Wiley)
[27] de Viry D, Casalboni M, Palummo M and Zema N 1990 *Solid State Commun.* **76** 1051
[28] Tippins H H 1970 *Phys. Rev.* B **1** 126
[29] Sirtlanov M R 1992 *J. Lumin.* **59** 101
[30] Casalboni M, Luci A, Grassano U M, Mill B V and Kaminskii A A 1994 *Phys. Rev.* B **49** 3781
[31] Balda R, Fernández J, Illarramendi M A, Arriandiaga M A, Adam J L and Lucas J 1991 *Phys. Rev.* B **44** 4759
[32] Henderson B, Yamaga M, Gao Y and O'Donnell K P 1992 *Phys. Rev.* B **46** 652
[33] Elejalde M J, Balda R, Fernández J, Macho E and Adam J L 1992 *Phys. Rev.* B **46** 5169